Politecnico di Torino

Porto Institutional Repository

[Article] Dynamics of spiral waves in a cardiac electromechanical model with a local electrical inhomogeneity

(Article begins on next page)

Spiral dynamics in a cardiac electromechanical model with a local electrical inhomogeneity

Luca Mesin[1, a)]

Department of Electronics and Telecommunications, Politecnico di Torino, Torino, Italy.

The electro–mechanical coupling in the heart is simulated by a three equation model, describing the electric potential, the recovery variable and the mechanical deformation, under the active strain hypothesis. The tissue is anisotropic and electrically inhomogeneous. The generation and dynamics of a spiral wave of excitation is studied.

Joint effect of electrical heterogeneity (e.g. induced by ischemia) and mechanical deformation is investigated for an anisotropic, quasi–incompressible model of cardiac electromechanical coupling (EMC) using the active strain approach and periodic boundary conditions. Under a specific stimulation protocol, the heterogeneity is able to induce spirals. The interplay between the dimension of the electrical inhomogeneity, the EMC and the mechano-electrical feedback provided by the stretch activated current determine the dynamics of the spiral wave of excitation.

I. INTRODUCTION

The contraction of the heart results from the integration of electrical, mechanical and biochemical processes at multiple spatial and temporal scales. Propagation of the action potential depends on coupling between cells, mediated by gap junctions. Even if such a coupling is heterogeneous within the myocardial wall[28], in healthy tissue, the action potential propagates in the form of a traveling pulse as if the medium was homogeneous. On the other hand, different activation patterns can originate when some perturbation occurs (at the gene, protein, cell or tissue scale[19]). For example, cardiac arrhythmias are characterized by rotating excitation waves[27], which resemble spirals occurring in some nonlinear media[37]. Different mechanisms for initiation of spirals have been proposed, but the most accepted one is related to local heterogeneities of the refractory properties of the tissue[9,26]. Such electrical inhomogeneities may be induced in the tissue as gap junctions are remodeled or as ionic concentrations are varied after ischemia and infarction[29], or during atrial fibrillation[35], or with aging[32].

Once elicited, spiral waves of action potential in the heart may have different dynamics[23]: stable rotation, with possible meandering or drift[25]; turbulent behavior (fibrillation)[25]; extinction[2,17]. The evolution of spirals is very important: the onset of turbulence is the main cause of cardiac depth[30] (most common cause of mortality in the industrialized world). It can arise from different instabilities. Alternans occur when the durations of successive excitation pulses alternate[23]. The onset of this instability is the factor that most probably determines ventricular fibrillation[11]. It arises if the action potential duration (APD) restitution curve (relation between APD and diastolic interval) has a slope larger than one[12].

Mathematical simulation may be useful to investigate the effect of the electrical and mechanical activities of the hearth on the dynamics of spiral waves in a healthy cardiac tissue or in the presence of pathological perturbations.

Many simulation studies have been conducted to assess the effect of the electrical coupling between cells on spiral dynamics. For example, a homogeneous reduction of cell coupling stabilizes spirals, due to the reduction of conduction velocity and increase of diastolic interval[23], which flatten the restitution curve. On the other hand, action potentials propagating on heterogeneous excitable tissues may have a complicated dynamics[5]: for example, transition from a stable plane wave to a spiral to potential blockage is observed in experiments and simulations as the degree of heterogeneity of cell coupling increases[33].

Simulations investigated also the effect on spiral dynamics of the cardiac mechanical activity[17,25], which is strongly coupled to the electrical one[4]. The contraction of the heart is controlled by action potentials propagating along the membrane of myocytes and the deformation induced on the tissue affects the propagation of the potential. Moreover, changes in tissue length induce a stretch activated current (SAC) determining a mechano–electrical feedback (MEF)[15]. Mechanics have a strong effect on spirals: their drift or breakup may be induced[17,25].

Usually, mechanical activity is described introducing an active stress[31]. Recently, another approach was also introduced[3,20], assuming that electrical potential dictates the active strain (not stress) of the muscle. This mod-

a)luca.mesin@polito.it

elling approach is finding some interesting applications and may have some advantages over the standard additive decomposition of the stress due to stability issues[17].

The dynamics of spirals on cardiac tissue models was usually investigated considering homogeneous tissues, or including heterogeneities, but neglecting mechanics. In this paper, a two dimensional (2D) anisotropic model of electromechanical coupling (EMC) is introduced within the active strain framework, including local electrical inhomogeneities with different geometries (modelling some of the features of a tissue affected by ischemia after acute infarction). Spiral wave generation and dynamics are studied. A specific stimulation protocol is adopted to exploit the longer refractory period of the inhomogeneous tissue to break a wavefront and to induce a spiral. Then, stimulation is stopped and spiral dynamics is investigated in relation to the geometry of the inhomogeneity, the strain of the contracted fibers (considering different contraction ratios) and the magnitude of the SAC (simulating different conductivities of the channels).

II. METHODS

An electro-mechanical model of cardiac tissue with a local inhomogeneity is subjected to a specific stimulation protocol which is able to induce a spiral wave (see Figure 1). Specifically, four pulses at constant frequency are used to get a stable condition; then, a pulse is delivered with a short delay from the previous one. The interval between the last two spikes is in between the refractory periods of the normal tissue and of the inhomogeneity, so that a traveling pulse is generated, but it is cut by the inhomogeneity. The dynamics of the spiral generated in this way is studied in relation to the properties of the simulated tissue.

The mechanics of the cardiac tissue is usually described decomposing the stress into passive and active components[31]. Here, a different approach is used[7]: the macroscopic excitable-contractile behavior of the tissue is described as a change in its rest state due to the contraction of active fibers.

The model is based on a 2D simulation tool already proposed in the literature[17], but introducing an electromechanical delay, choosing physiological parameters and describing an electrical inhomogeneity. Electrical parameters for the inhomogeneity are chosen to simulate some of the main perturbations induced in a tissue affected by ischemia after an acute infarction: the excitability is reduced with respect to that of a normal tissue, recovery dynamics is modified to account for a shortening of the duration of the action potential and for the increase in the refractory period, and the rest potential is increased to simulate depolarization[2]. On the other hand, mechanical properties of the heterogeneous region are the same as for the normal tissue.

The model complexity is kept to a minimum, considering simple constitutive assumptions for the tissue and
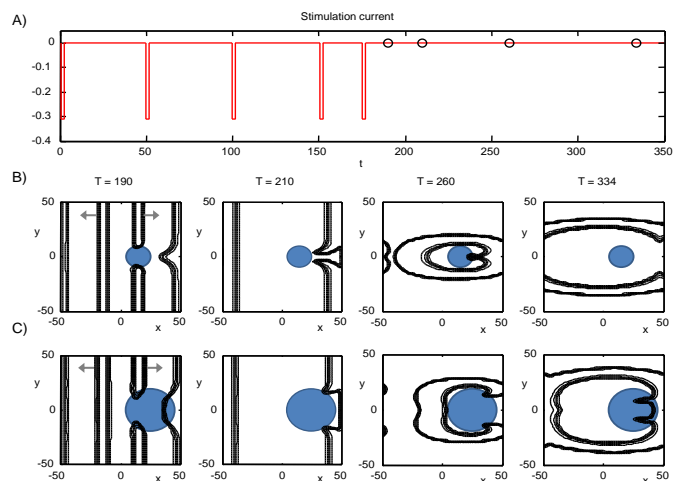

FIG. 1. Stimulation protocol and onset of spirals. The stimulation protocol is shown in A) for the first 350 time units, indicating with small circles the instants of time considered in B) and C). Example of simulated potential (contour line plot) corresponding to different time instants (after the last stimulation, during the onset of the spiral and at the beginning of the second turn). Two cases are considered: B) rigid tissue with a small circular inhomogeneity, C) deformable tissue with a large circular inhomogeneity (contraction ratio $\beta = 0.1$, conductivity of SACs $G_s = 0.1$). Grey arrows in B) and C), left panel, indicate the direction of propagation of the action potential.

a phenomenological description of the electrical activity, but representing important phenomena like EMC, MEF and ADP restitution property, which are expected to affect the dynamics of spiral waves.

A. Mechanical model

Every material point is labeled by its position in a relaxed configuration at time $t = 0$. The motion of the point $\mathbf{X}$ is defined by the vectorial map $\mathbf{x} = \mathbf{x}(\mathbf{X}, t)$. The gradient of this function is the tensor gradient of deformation:

$$\mathbf{F} = \mathrm{Grad}\,\mathbf{x}\,, \quad F_{ij} = \frac{\partial x_i}{\partial X_j}, \quad 1 \leq i, j \leq 3 \quad (1)$$

The visible deformation gradient $\mathbf{F}$ is decomposed into an active ($\mathbf{F}_o$) and a passive ($\mathbf{F}_e$) component

$$\mathbf{F} = \mathbf{F}_e \mathbf{F}_o \quad (2)$$

which is a theoretical decoupling that associates the micro–scale dynamics (due to the contraction of the myocytes) to the macro–scale continuum mechanics. The active deformation prescribes the contraction of the myocytes along their own direction $\mathbf{n}$

$$\mathbf{F}_o = \mathbf{1} + \gamma(v)\mathbf{n} \otimes \mathbf{n}, \quad (3)$$
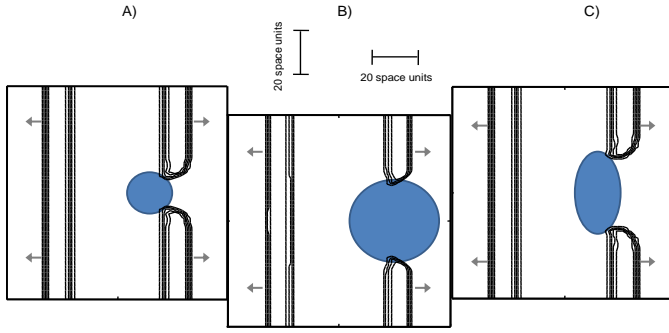
FIG. 2. Example of simulated data corresponding to different inhomogeneities (with the shape of a small circle A, a large circle B or an ellipse C), but with constant simulation parameters (contraction ratio $\beta = 0.1$, conductivity of SACs $G_s = 0.15$). Contour lines are shown for the potential at time sample number 200. The propagating front is broken by the refractory inhomogeneous tissue. Grey arrows in B) and C), left panel, indicate the direction of propagation of the action potential.
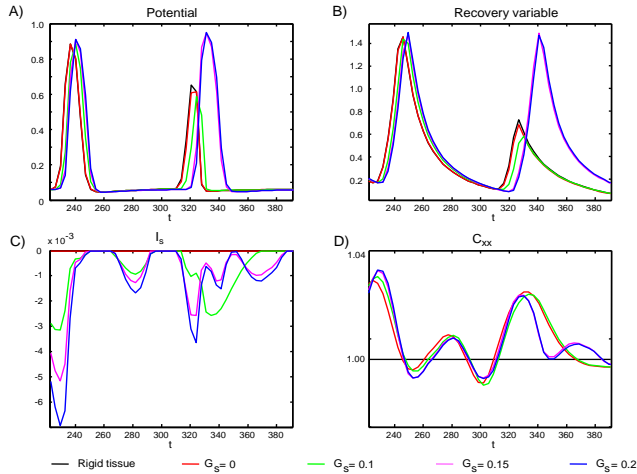

FIG. 3. Time evolution of some electrical and mechanical variables in the center of a small circular inhomogeneity in cases in which the broken wave is converted into a spiral or it extinguishes after a single turn. A) Potential, B) recovery variable, C) stretch activated current, D) component xx of the Cauchy-Green stress tensor.

where $\mathbf{1}$ is the identity matrix, $\otimes$ indicates tensorial product and v is the electric potential. The activation function $\gamma(v)$ is the convolution of the potential with an exponential with time constant $\tau = 10$, modeling an electromechanical delay of about 10 time units and increasing the time support of the mechanical response with respect
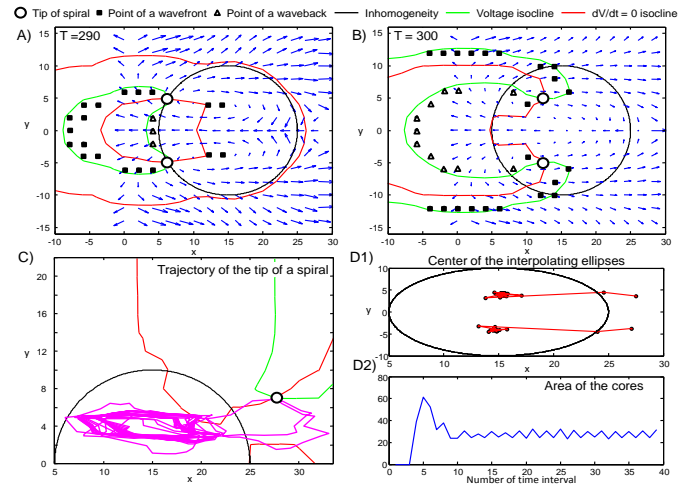

FIG. 4. Example of processing of simulated data ($\beta = 0.1$, $G_s = 0.15$, small inhomogeneity). The isocline of constant membrane voltage (equal to 0.15) and the line where the time derivative of the potential vanishes are indicated. Their intersection is the identified tip of the spiral, indicated with a circle in A), B) and C). The points belonging to a wavefront or a waveback are also depicted in A) and B), together with the flow of the potential in a portion of tissue around the tip of the spiral (optical flow is estimated by a multi-image approach using 20 images close in time to the considered one, which is for $T = 290$ and $T = 300$, in A and B, respectively). The trajectory of the tip of the spiral in the upper semi-plane is shown in C), together with the boundary of the inhomogeneity and the potential isoclines. Centers and area of the cores described by the tip of the spirals for each turn are shown in D1) and D2), respectively.

to the electrical activation

$$\gamma(v) = -\beta\, v * u(t)\, e^{-\frac{t}{\tau}}, \tag{4}$$

where $u(t)$ is the step function, $*$ indicates convolution operator and β is the contraction ratio. The stress tensor is the derivative of the strain energy of a neo–Hookean material, assumed to depend on the deformation at the macro–scale

$$W(\mathbf{F}_e) = \frac{\mu}{2}\left(tr\mathbf{F}_e\mathbf{F}_e^T - 2\right) + \frac{\alpha}{2}(\det \mathbf{F} - 1)^2, \tag{5}$$

where the last term penalizes compressibility. Force balance is written in the reference configuration by a pullback[14]:

$$\text{Div}\left(\mu J_o \mathbf{F}\mathbf{F}_o^{-1}\mathbf{F}_o^{-T} + \alpha J(J - 1)\mathbf{F}^{-T}\right) = 0. \tag{6}$$

The values of the parameters are $\mu = 2000$ and $\alpha = 1000$. The mechanical properties are taken homogeneous, regardless of the presence of an electrically inhomogeneous region.

B. Electrical model

Muscle contraction is induced by a macroscopic electrical signal which is determined by ionic fluxes at a smaller

length scale controlled by channels with conductivity depending on the transmembrane potential[22]. The effect of ionic fluxes on potential v is here represented by a phenomenological model[1] accounting for the restitution curve, including a fast cubic reaction term and a slow recovery variable w

$$
\begin{cases}
\dfrac{\partial v}{\partial t} - \text{Div}\left(\mathbf{F}^{-1}\mathbf{D}\mathbf{F}^{-T}\text{Grad}\,v\right) = \\
\qquad = -kv(v-\alpha_1)(v-1) - wv - I_s(v) - I_{stim}(t) \\
\dfrac{\partial w}{\partial t} = \left(\varepsilon + \dfrac{\mu_1 w}{\mu_2 + v}\right)\left(-w - kv(v - \alpha_2 - 1)\right).
\end{cases}
\tag{7}
$$

Here $\mathbf{D}$ is the diffusion tensor (ratio between fiber conductivity and specific cell membrane capacitance), $I_s(v)$ is the SAC

$$
I_s(v) = \begin{cases}
G_s(\mathbf{C_{nn}} - 1)\,(v - 1) & \text{if } \mathbf{C_{nn}} > 1 \\
0 & \text{if } \mathbf{C_{nn}} \le 1
\end{cases}
\tag{8}
$$

where G_s is the conductance of SAC channels and $\mathbf{C_{nn}}$ is the component of the Cauchy-Green stress tensor aligned to the direction of the fibers. Finally, the function $I_{stim}(t)$ in equation (7) is the stimulation current, which is constituted by 4 rectangular pulses (duration 1.5 time units) with delay 50 units, plus a pulse delayed 25 units from the last (Figure 1A). Stimulation is provided in the vertical stripe $-10 < X < 10$, with a maximum in $X = 0$ and a linear decrease away from this line. A diagonal diffusion tensor is considered. Conductivity is 5 times larger in the direction longitudinal to the fibers than in the transversal one[10] ($D_{xx} = 2$, $D_{yy} = 0.4$ for normal tissue). Conductivity of the heterogeneous region is decreased of 30% (similar variation are found during the initial phase of ischemia[34]).

The values of the parameters in (7) for normal tissue[1] are $k = 8$, $\alpha_1 = \alpha_2 = 0.15$, $\varepsilon = 0.002$, $\mu_1 = 0.2$, $\mu_2 = 0.3$. The inhomogeneous tissue has a shorter action potential with respect to that of a normal tissue (duration about one half), a reduced excitability (a 25% lower conductivity of Na^+ channels is found on ischemic tissue[8]), a decreased resting potential[8] and an increased refractory period[2]. These properties are simulated by increasing the rest potential to the non dimensional value 0.05 and choosing the following values of parameters of the Aliev-Panfilov model: $k = 8$, $\alpha_1 = 0.2$, $\alpha_2 = 0.6$, $\varepsilon = 0.002$, $\mu_1 = 0.1$, $\mu_2 = 1.2$.

The model has dimensionless units, but dimensional values may be obtained[1] by transforming the non–dimensional potential (varying between 0 and 1) by the linear map E $= 100\,v - 80$ mV and multiplying the time unit by 12.9 ms. Assuming that conduction velocity is $0.4\ m/s$,[10] the simulation of a traveling impulse on a homogeneous tissue indicates that the non–dimensional space unit corresponds to about 3 mm.

C. Numerical issues

The numerical domain is a square, with side length 100 (about 30 cm, in dimensional units) and centered at the origin of a Cartesian coordinates system. Periodic conditions are assumed for both the mechanical and the electrical problems. The fibers are supposed to be aligned along the X direction.

The different space and time scales of the mechanical and the electrical problems suggest to introduce different discretization steps (for the mechanical problem $\Delta x_{mech} = 4$, $\Delta t_{mech} = 1$; for the electrical problem $\Delta x_{electr} = 1$, $\Delta t_{electr} = 0.04$; nevertheless, for memory saving, electric data are saved with $\Delta x_{electr}^{save} = 2$, $\Delta t_{electr}^{save} = 2$ and such undersampled data are processed and shown in the following). The mechanical and electrical equations (6) and (??) are decoupled and linearized for each time step. The finite difference discretization of the mechanical problem is solved using the Gaussian elimination Matlab routine optimized for sparse matrices. The electrical problem is solved by a time marching implicit method (see[17] for details).

Two circular and an ellipsoidal local inhomogeneities are considered in different sets of simulations (including a smooth transition region with thickness about 4 space units): the small circular inhomogeneity has a radius of 10 space units and the center is in $(X = 15, Y = 0)$; the large circular inhomogeneity has radius equal to 20 space units and the center is in $(X = 25, Y = 0)$; the ellipsoidal inhomogeneity has the shape of an ellipse with X axis of 10 and Y axis of 20 space units and the center is in $(X = 15, Y = 0)$ (see Figure 2). The centers of the inhomogeneities are located in order that the distance from the center of the domain $X = 0$ (where the stimulus is provided) to the nearest border of the inhomogeneities is constant (equal to 5 space units).

The parameters to be varied in different simulations are the contraction ratio β (in the range $10 - 20\%$)[25] and the conductance G_s of the SAC (range $0 - 0.2$). Numerical solution is computed till $t = 2000$ (≈ 26 s).

D. Signal processing

The tip of a spiral is a phase singularity. It is estimated as the intersection point of an isocline of constant membrane voltage (equal to 0.15) and a line where the time derivative of the potential vanishes[38]. In order to estimate the trajectories of the tips of the spirals, each point identified for each time sample is associated to the spiral with closest trajectory (if it is closer than 4 space units), or a new spiral is originated by points which are not classified or are too distant from the already computed trajectories. Note that the distance between points is computed considering periodicity (so that, a spiral exiting from the left/bottom border of the domain enters from the right/top side).

In all the simulations, two main trajectories, symmetrical with respect to the X axis, are identified, together with some spurious points which are neglected. Only the trajectory in the domain $y > 0$ is considered for further analysis.

The motion of the tips of simulated spirals is investigated in time intervals during which spirals perform single rotations. To identify such intervals, the potential on the center of the inhomogeneity is considered. Indeed, the tips of stable spirals have trajectories which develop inside the inhomogeneity and a front of potential passes across the center of the inhomogeneity one time for each rotation. The time locations of local maximal values of the potential (excluding possible points below a threshold of 0.7) are used to estimate the time intervals in which spirals performed single turns of rotation. The mean frequency of spiral rotation is estimated from the mean duration of such time intervals. Moreover, the portion of trajectory followed by the tip of a spiral during a rotation is interpolated with an ellipse, using the analytical method of Chaudhuri and Kundu[6] (estimating the radius and the center of a circle) after rescaling the points with respect to their range. Given the interpolating ellipses for each rotation of the spiral, interesting parameters are available to characterize the dynamics: the two axes of the interpolation ellipses, the perimeter and the area of the cores of rotating spiral waves and the trajectory of the center of the cores.

Moreover, wave fronts and wave back are computed. Voltage maps for each time sample are binarized with a cutoff value of 50%. Then, subsequent maps are subtracted, obtaining the fronts[16]. The number of border points identified by such a procedure is considered as indicative of the complexity of the voltage distribution.

To test if the specific properties of the simulated tissue have a significant effect on the estimated variables, three-way analysis of variance (ANOVA) is performed considering different variables (mean frequency, mean area of the cores, length of the trajectory of a tip, length of the trajectory of the cores, mean axes of the interpolation ellipses, number of points of the fronts) as a function of the following factors: geometry of the inhomogeneity (small circle, large circle, ellipse), contraction ratio (β) and conductivity of the SAC (G_s). The significance level is set to $p = 0.05$ or to $p = 0.01$ (highly significant). When ANOVA indicates that a factor affects significantly a variable, Newman-Keuls post-hoc test is used to make pairwise comparisons.

III. RESULTS

Figure 1 shows how the stimulation protocol (in 1A) can determine the onset of spiral waves, in two tissues with different properties: a rigid tissue with a small circular inhomogeneity is considered in 1B, a deformable tissue with a large circular inhomogeneity in 1C. The stimulation protocol is shown in 1A for the first 300 time units. The simulated potential is shown in contour line plots in 1B and 1C corresponding to different time instants (indicated by circles in 1A): the first is after the last stimulation, when the last traveling front is broken by the inhomogeneity which is still refractory, unlike the normal tissue; in the second time instant, the potential starts to curl; in the third, the spiral is formed (actually, two spirals, symmetrical with respect to the X axis); the last time instant is at the beginning of the second turn of the spiral. In the case of a rigid tissue, the spiral extinguishes after the first turn. The extinction of the spirals after a single turn was also observed in the case of small inhomogeneity, for contraction ratio $\beta = 0.1$ and $G_s \leq 0.1$, for $\beta = 0.15$ and $G_s \leq 0.05$, and for $\beta = 0.2$ and $G_s \leq 0.05$. On the contrary, in the case of the deformable tissue with a large circular inhomogeneity shown in 1C, periodic spirals develop.

Figure 2 shows the onset of spirals of action potential on tissues with different inhomogeneities, but with constant simulation parameters. Contour lines are shown for the potential at time sample number 200. The propagating front is broken by the refractory inhomogeneous tissue and the spirals start their dynamics, which extinguishes for the inhomogeneity considered in 2A, whereas it is periodic for the other two inhomogeneities which determine a larger break in the traveling front.

Figure 3 shows different variables (potential, recovery variable, SAC and component xx of the Cauchy-Green stress tensor) computed in the center of the small circular inhomogeneity in cases in which the broken wave is converted into a spiral or it extinguishes after a single turn. The considered time interval allows to see the potential for the first and the second turn of the spiral. When the tissue is rigid, or it is deformable but with a low conductivity G_s of the SAC, the second re-entrant wave is under threshold and extinguishes. When the SAC is sufficiently high (as shown in 3C), the stimulation is sufficient to excite the tissue, even if it is still relatively refractory.

Figure 4 shows an example of processing of simulated data. The isocline of constant membrane voltage (equal to 0.15) and the line where the time derivative of the potential vanishes are indicated in 4A, 4B and 4C. Their intersection is the identified tip of the spiral, indicated with a circle in 4A, 4B and 4C. The points belonging to a wavefront or a waveback are also depicted in 4A and 4B, together with the flow of the potential in a portion of tissue around the tip of the spiral. To estimate the flow of the potential, a multi-image generalization of the Lucas-Kanede technique[18] was applied, using 20 images close in time to the considered one, which is for $T = 290$ and $T = 300$, in 4A and 4B, respectively. The trajectory of the tip of the spiral in the upper semi-plane is shown in 4C, together with the boundary of the inhomogeneity and the potential isoclines at the onset of the spiral. The tip of the spiral is initially out of the inhomogeneity. Then, it moves toward the inhomogeneity, it enters and then rotates within it, describing an ellipse with largest

axis along the fiber. Centers and area of the cores described by the tip of the spirals for each turn are shown in 4D1 and 4D2, respectively. Again, the trajectory of the tip is shown to enter the inhomogeneity, where it rotates around a center which stays close to the middle of the heterogeneity (Figure 4D1). The area of the cores converges to an approximately constant value, after the first turns in which the tip is drifting (Figure 4D2).

Figure 5 shows the spiral dynamics in a specific case in which the spirals move out of the inhomogeneous region and drift away till reaching the upper/lower border of the domain. There, the two spirals interact, due to the periodic boundary conditions, and annihilation occurs. The extinction of the spirals is related to a high value of G_s, somehow in contrast (even if the phenomena are very different) to what shown in Figure 3, where an increasing SAC appears to have a stabilizing effect on spiral formation. The overall indication is that intermediate values of G_s are related to stable spiral dynamics. The potential is shown in 5A in four time instants: in the first, the traveling front is just broken; in the second and third, the spiral is developed, its tip is out of the inhomogeneity and is drifting; in the last time instant, the spirals disappear and a traveling wave is formed. The estimated trajectories of the tips of the two symmetric spiral waves are shown in 5B, where it is clear that the tips, after the development of the spirals, are not able to remain within the inhomogeneity and then drift toward a boundary of the domain. In Figure 5C, the component of the Cauchy-Green stress tensor along the direction of the fibers, in the center of the inhomogeneity is shown. After the first periodic traveling waves induced by the stimulation pulses (corresponding to periodic stretch and shortening), the spirals are generated, which determine an aperiodic strain in the center of the inhomogeneity. Then, a periodic traveling wave develops (as shown in 5A, last considered time instant) and the strain of the tissue becomes periodic.

Figure 6 shows mean and standard errors of the variables extracted from the simulated spirals considering different inhomogeneities. Statistically significant differences are indicated. The differences are almost always highly significant. Specifically, the smallest circular inhomogeneity is associated always to statistically shorter trajectories of the tip of the spirals with respect to the other simulated inhomogeneities. This is also associated to a smaller core and a shorter trajectory of the cores. Indeed, a stable spiral rotates with the tip anchored inside the inhomogeneity, so that its trajectory is forced to develop within a smaller region in the case of the smallest inhomogeneity simulated. As a consequence, the frequency of the spiral rotation is higher for the smallest inhomogeneity (note that, for example, a frequency of 0.036 corresponds to about 2.8 Hz or 168 pulses per minutes in dimensional units). Sometimes, the time needed for the potential to re-enter a point is so small that the potential extinguishes (as shown in Figures 1B and 3). Also the wavefronts and wavebacks are shorter for the
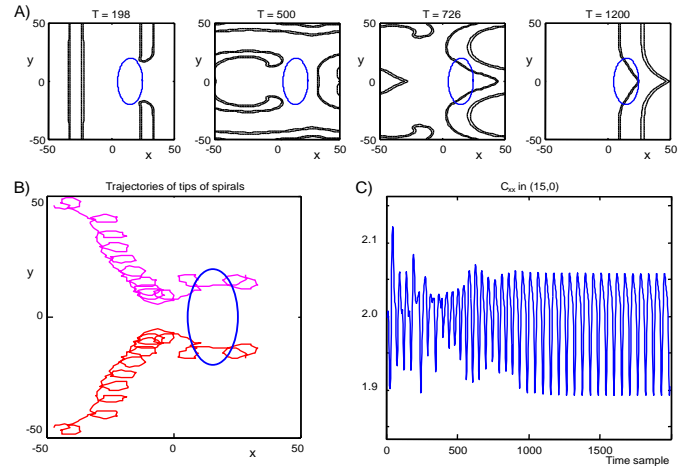

FIG. 5. Spiral dynamics in the case of elliptic inhomogeneity, with contraction ratio $\beta = 0.3$ and conductivity of the SAC $G_s = 0.2$. A) Potential in different time instants represented in contour plots. B) Trajectories of the tips of two symmetric spiral waves. C) The component along the X axis of the Cauchy-Green stress tensor in the center of the inhomogeneity.

smallest inhomogeneity.

Figure 7 shows mean and standard errors of the same variables as in Figure 6, but considering different values of conductivities of the SAC. In this case, only a few groups are statistically different, and rarely the differences are highly significant. Nevertheless, some trends are quite consistent: the frequency, the number of wavefront or waveback pixels, the length of trajectory of the tip or of the cores, the area and the axes of the interpolating ellipses (mainly the Y-axis, in relative terms) increase for increasing conductivity of the SAC.

No significant differences are found when data are grouped with respect to the contraction ratio β. Only trends are obtained, resembling those shown in Figure 7 (not shown results).

IV. DISCUSSION

A. Elements of innovation with respect to the literature

Effects of electrical inhomogeneities[23,33] and of mechanical deformation[17,25] on spiral dynamics in the heart are usually simulated separately in literature. In this paper, the joint effect of electrical heterogeneity and mechanical deformation is studied.

A model of cardiac EMC is considered describing the mechanical and electrical anisotropy induced by the fibers (this detail is sometime neglected in literature). From the mechanical viewpoint, the simulated tissue is quasi–incompressible and the active strain hypothesis is assumed, in contrast with much of the literature, where an active stress is usually introduced.
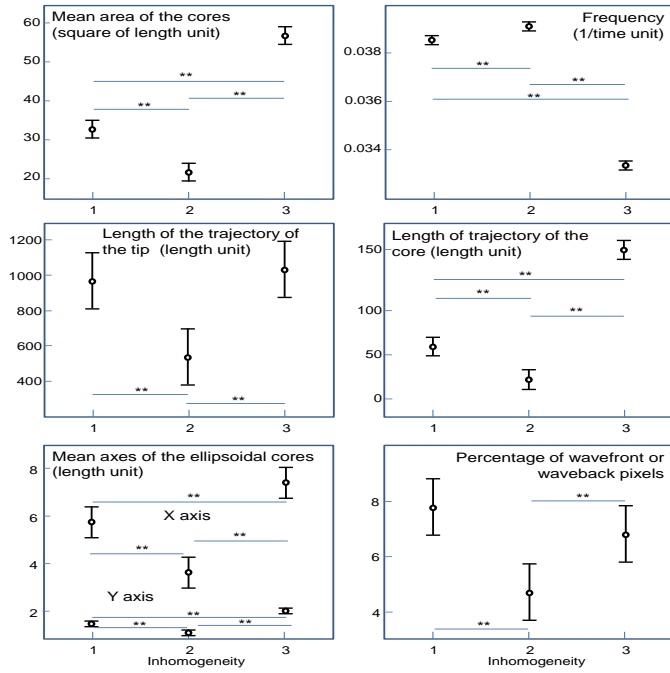
FIG. 6. Statistical analysis (mean and standard error) with respect to the factor inhomogeneity (1. ellipse, 2. small circle, 3. large circle).
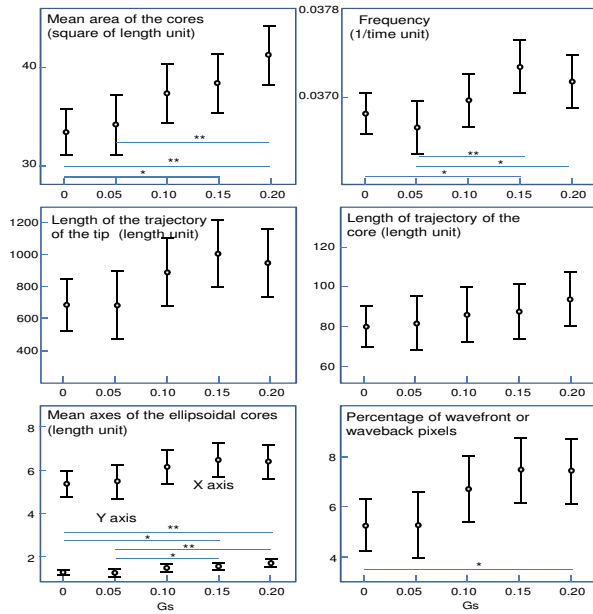

FIG. 7. Statistical analysis (mean and standard error) with respect to the factor G_s.

(as in Figure 1), they collide (due to periodicity of the conditions) and annihilate, as if the tissue was a closed surface (as the heart is). It is worth noticing that the simulated tissue is not a torus, as in such a case curvature effects should be considered. From the mechanical point of view, periodic conditions also influence the dynamics, as the contraction of a portion of the tissue (e.g. induced by two traveling fronts propagating in opposite direction) distributes on the whole simulated cardiac medium, without interacting with other surrounding tissues (which would have properties which would affect the results of the simulation).

The choice of periodic boundary conditions affects also the dynamics of a spiral wave of action potential: as it interacts with waves entering again the domain from the boundary, it could be expected that the activation pattern could be richer than in the case in which traveling waves were allowed to exit the domain.

B. Formation of a spiral

The simulated local inhomogeneities are able to break a traveling wave of potential and induce re-entrance. A region with longer refractory period than the neighboring cells is thought to have a key role in wave breaking[9,26]: when a wave travels across a tissue with heterogeneous refractory properties, a pattern of excitable and refractory regions forms, that can break an incoming new activation wave. This broken wave may start curling from the open edges as soon as the tissue with prolonged refractory period is again excitable, inducing a spiral from a traveling pulse or contributing to the onset of turbulence from spirals.

C. Discussion of results

The interplay between EMC, MEF and inhomogeneity geometry determine the final equilibrium of the dynamics of spirals induced by the inhomogeneity (under a specific stimulation protocol). Specifically, contraction ratio and stretch activated channels have an important role. In the case of the smallest simulated inhomogeneity, a sufficiently large conductivity of SACs is required to sustain a periodic rotation of spirals, which otherwise extinguish after the first rotation. The minimal value of conductivity required to get periodic rotations is lower for a larger value of contraction ratio.

When stable rotations are obtained, they are anchored to the inhomogeneity. This is in line with an experimental study[13], where local heterogeneity with slow conduction have been produced with a reversible process. Stimulating the tissue with a high frequency (in order to produce close propagating waves), spiral waves anchored to the local inhomogeneity could be produced.

In the case of the elliptic inhomogeneity, the greatest simulated contraction ratio and the largest value of

conductivity of SACs induce the unbinding from the inhomogeneity, a drift of the spirals toward the upper or lower boundary and the annihilation of each spiral with the other symmetrical wave after a few turns, determining their extinction (Figure 5). This large drift is possible only for a high value of conductivity of the SAC, in line with other simulation studies[25], where SAC was indicated as the main factor driving spiral drift. A traveling wave is finally generated after the extinction of the spirals. It travels periodically due to the assumed boundary conditions (this is in line with a previous simulation study[17], where spirals dynamics were studied assuming periodic conditions).

When stable spirals are obtained, the specific parameters chosen (contraction ratio and conductivity of SAC) determine variations in spiral dynamics, as reflected by statistically significant variations of variables (like the trajectory of the tip of the spiral, or the geometry of the cores described by the tip during rotations) considered in the literature to describe spiral dynamics. In particular, the trajectory of the tip of the spiral lengthens and the area of the cores increases as the conductivity of the SAC increases. This could force the tip to exit from the inhomogeneity and to drift away, as in the case shown in Figure 5.

The conductivity G_s of the SACs is indicated by the statistical analysis as the main factor affecting spiral dynamics, whereas the mere contraction has only a relative marginal effect.

D. Limitations

The model considered is very simple, compared to the physiological tissue. Main limitations are the followings:

- mechanical heterogeneity due to the ischemic region[36] is neglected (the approximation can be good during the acute phase of ischemia);

- phenomenological description of excitation mechanism (which could be properly described by considering different ionic currents[22]; including the ion Ca^{2+} would allow to represent more closely the onset of mechanical contraction, which is here represented by a simple phenomenological model linking the contraction directly to the action potential);

- simple 2D geometry;

- only EMC is considered, neglecting other phenomena, e.g. the interaction between cardiac walls and blood.

E. Future works

The specific role of mechanics and excitation could be further discussed, possibly in light of a longer simulated time range, with different parameters (e.g. electromechanical delay), or with more detailed models of the ionic fluxes.

In literature, Dirichlet[24,25], Neumann[21], Robin[3], periodic[17] boundary conditions are considered for the mechanics while Neumann (insulated)[25] or periodic conditions[17] are assumed for the electrical problem. The effect of boundary conditions on wave dynamics should be further investigated.

The use of multi-image optical flow techniques could be further exploited to extract parameters from simulated maps of action potential on two dimensional models of a cardiac tissue.

F. Conclusion

EMC coupling and MEF provided by SAC have great importance in spiral dynamics.

[1]R.R. Aliev, A.V. Panfilov, "A simple two-variable model of cardiac excitation," Chaos, Solitons & Fractals, **7**, pp. 293–301 (1996).

[2]R.R. Aliev, A.V. Panfilov, "Modeling of Heart Excitation Patterns caused by a Local Inhomogeneity," J. theor. Biol., **181**, pp. 33-40 (1996).

[3]D. Ambrosi, G. Arioli, F. Nobile, and A. Quarteroni, "Electromechanical coupling in cardiac dynamics: the active strain approach," SIAM J. Appl. Math., **71(2)**, pp. 605-621 (2011).

[4]D.M. Bers, "Cardiac excitation-contraction coupling," Nature, **415**, pp. 198–205 (2002).

[5]G. Bub, A. Shrier, "Propagation through heterogeneous substrates in simple excitable media models", Chaos, **12**, pp. 747–753 (2002).

[6]B.B. Chaudhuri, P. Kundu, "Optimum circular fit to weighted data in multidimensional space," Pattern Recogn. Lett. **14**, pp. 16 (1993).

[7]C. Cherubini, S. Filippi, P. Nardinocchi, and L. Teresi, "An electromechanical model of cardiac tissue: Constitutive issues and electrophysiological effects," Progr. Biophys. Molec. Biol., **97**, pp. 562–573 (2008).

[8]A. Cimponeriu, C.F. Starmer, and A. Bezerianos, "A Theoretical Analysis of Acute Ischemia and Infraction Using ECG Reconstruction on a 2D Model of Myocardium," IEEE Trans Biomed Eng, **48**(1), pp. 1–14 (2001).

[9]R.H. Clayton and P. Taggart, "Regional differences in APD restitution can initiate wavebreak and re-entry in cardiac tissue: A computational study," Biomed. Eng. Online, **4**, pp. 54: 1–14 (2005).

[10]R.H. Clayton, O. Bernus, E.M. Cherry, H. Dierckx, F.H. Fenton, L. Mirabella, A.V. Panfilov, F.B. Sachse, G. Seemann, and H. Zhang, "Models of cardiac tissue electrophysiology: Progress, challenges and open questions," Prog Biophys Mol Biol vol. **104**(1-3), pp. 22–48 (2011).

[11]A. Garfinkel, Y.H. Kim, O. Voroshilovsky, Z. Qu, J.R. Kil, M.H. Lee, H.S. Karagueuzian, J.N. Weiss, and P.S. Chen, "Preventing ventricular fibrillation by flattening cardiac restitution," Proc. Nat Acad Sci. **97**, pp. 6061–6066 (and cover) (2000).

[12]M.R. Guevara, G. Ward, A. Shrier, and L. Glass, "Electrical alternans and period-doubling bifurcations," IEEE Computers in Cardiology, **562**, pp. 167–170 (1984).

[13]J.W. Lin , L. Garber, Y.R. Qi, M.G. Chang, J. Cysyk, L. Tung, "Region of slowed conduction acts as core for spiral wave reentry in cardiac cell monolayers," Am J Physiol Heart Circ Physiol **294**, pp. H58H65 (2008).

[14]I-Shih Liu, *Continuum Mechanics*, Springer, 2002.

[15] P. Kohl, K. Day, and D. Noble, "Cellular mechanisms of cardiac mechano-electric feedback in a mathematical model," Can J Cardiol. **14**(1), pp. 111–119 (1998).

[16] R. Mandapati, Y. Asano, W.T. Baxter, R.A. Gray, J.M. Davidenko, J. Jalife, "Quantification of effects of global ischemia on dynamics of ventricular fibrillation in isolated rabbit heart," Circulation **98**, pp. 1688-1696 (1998).

[17] L. Mesin and D. Ambrosi, "Spiral waves on a contractile tissue," Eur. Phys. J. Plus **126**, pp. 21: 1–13 (2011).

[18] L. Mesin, "Short range tracking of rainy clouds by multi-image flow processing of X-band radar data," EURASIP Journal on Advances in Signal Processing 2011: 67.

[19] J.D. Moreno and C.E. Clancy, "Using computational modeling to predict arrhythmogenesis and antiarrhythmic therapy," Drug Discov Today Dis Models. **6**(3), pp. 71-84 (2009).

[20] P. Nardinocchi, L. Teresi, "On the Active Response of Soft Living Tissues," J. Elasticity, **88**, pp. 27-39 (2007).

[21] M.P. Nash and A.V. Panfilov, "Electromechanical model of excitable tissue to study reentrant cardiac arrhythmias," Prog Biophys Mol Biol. **85**(2-3), pp. 501–522 (2004).

[22] D. Noble, "Modeling the heart," Physiology **19**, pp. 191197 (2004).

[23] A.V. Panfilov, "Spiral Breakup in an Array of Coupled Cells: The Role of the Intercellular Conductance," Phys. Rev. Lett., **88**(11), pp. 118101: 1–4 (2002).

[24] Panfilov AV, Keldermann RH and Nash MP, Self–organized pacemakers in a coupled reaction–diffusion–mechanics system, Phys. Rev. Lett., 95:258104 (2005).

[25] A.V. Panfilov, R.H. Keldermann, and M.P. Nash , "Drift and breakup of spiral waves in reaction–diffusion– mechanics systems," Proc. Natl. Acad. Sci. USA, **104**, pp. 7922–7926 (2007).

[26] G.B. Makkers van der Deijl and A.V. Panfilov, "Formation of fast spirals on heterogeneities of an excitable medium," Phys.Rev.E., **78**, pp. 012901: 1–4 (2008).

[27] A.M. Pertsov, J.M. Davidenko, R. Salomonsz, W.T. Baxter, and J. Jalife, "Spiral waves of excitation underlie reentrant activity in isolated cardiac muscle," Circulation Research, **72**, pp. 631–650 (1993).

[28] S. Poelzing, F.G. Akar, E. Baron, and D.S. Rosenbaum, "Heterogeneous connexin43 expression produces electrophysiological heterogeneities across ventricular wall," Am J Physiol Heart Circ Physiol, **286**, pp. H2001-H2009 (2004).

[29] J.M.B. Pinto and P.A. Boyden, "Electrical remodeling in ischemia and infarction," Cardiovascular Research, **42**, pp. 284-297 (1999).

[30] R. Pool, "Heart like a wheel," Science, **247**, pp. 1294-1295 (1990).

[31] N.P. Smith, D.P. Nickerson, E.J. Crampin, P.J. Hunter, "Multiscale computational modelling of the heart," Acta Numerica, pp. 371431 (2004).

[32] M.S. Spach and P.C. Dolber PC, "Relating extracellular potentials and their derivatives to anisotropic propagation at a microscopic level in human cardiac muscle. Evidence for electrical uncoupling of side-to-side fiber connections with increasing age," Circ Res., **58**(3), pp. 356–371 (1986).

[33] B.E. Steinberg, L. Glass, A. Shrier, and G. Bub, "The role of heterogeneities and intercellular coupling in wave propagation in cardiac tissue," Philos Transact A Math Phys Eng Sci., **15**(364-1842), pp. 1299–1311 (2006).

[34] J.G. Stinstra, S. Shome, B. Hopenfeld, R.S. MacLeod, "Modelling passive cardiac conductivity during ischemia," Med. Biol. Eng. Comput., **43**, pp. 776-782 (2005).

[35] H.M. Van der Velden, J. Ausma, M.B. Rook, A.J. Hellemons, T.A. van Veen, M.A. Allessie, and H.J. Jongsma, "Gap junctional remodeling in relation to stabilization of atrial fibrillation in the goat," Cardiovasc Res, **46**, pp. 476-486 (2000).

[36] C.P.F. Weidemann, C. Dommke, V. Bito, F.R. Heinzel, J. D'hooge, K.R. Sipido, G.R. Sutherland, and B. Bijnens, "Mechanisms of postsystolic thickening in ischemic myocardium: mathematical modelling and comparison with experimental ischemic substrates," Ultrasound Med Biol, **33**(12), pp. 1963–1970 (2007).

[37] A.T. Winfree and S.H. Strogatz, "Organising centres for three-dimensional chemical waves," Nature, **311**, pp. 611–615 (1984).

[38] E.A.Zhuchkova, R.H. Clayton. "Methods for identifying and tracking phase singularities in computational models of reentrant fibrillation," Lecture Notes in Computer Science, **3504**, pp. 246–255 (2005).